ELSEVIER

Polymer 43 (2002) 3647–3652

polymer

www.elsevier.com/locate/polymer

Order–disorder transition of micellar aqueous solution of hydrophobically modified polyethyleneglycol (C12E25)

Ritsuko Yamazaki[a,*], Katsuhiro Inomata[b,1], Takuhei Nose[b,2]

[a]*Skin Care Laboratory, Kao Corporation, 2-1-3 Bunka, Sumida-ku, Tokyo 131-8501, Japan*
[b]*Department of Polymer Chemistry, Tokyo Institute of Technology, 2-12-1 Ookayama, Meguro-ku, Tokyo 152-8552, Japan*

Received 13 November 2001; received in revised form 21 February 2002; accepted 1 March 2002

Abstract

Aggregation behavior of hydrophobically modified ethyleneglycol oligomer, poly(ethylene glycol) monododecyl ether (C12E25), in aqueous solution has been studied in wide ranges of concentration and temperature by means of light scattering, X-ray scattering, and linear-viscoelastic measurements. C12E25 forms stable micelles in dilute solution. It is found that the micellar solution exhibits the sol–gel transition accompanied with disorder-to-order structural transition as increasing concentration at lower temperatures, or with decreasing temperature at higher concentrations. The transition concentration is located around 30 wt% irrespective of temperature, while the transition temperature is about 56 °C independent of concentration. In the gel region, the micellar particles form a long-range order structure of body-centered cubic lattice. © 2002 Elsevier Science Ltd. All rights reserved.

Keywords: Poly(ethylene glycol) monododecyl ether; Sol–gel transition; Order–disorder transition

1. Introduction

Hydrophobically modified poly(ethylene glycol) (PEG) is widely used as a surfactant, taking advantage of easy control of its hydrophobicity by changing the alkyl group species and ethyleneoxide (EO) chain length. Their structures and properties in aqueous solution have extensively been studied [1–8] by means of static and dynamic light scattering [9–16], NMR, and others [17–20]. Most of the studies have been devoted to modified PEGs with relatively short EO chains to reveal their phase diagrams and aggregation behavior in aqueous solution.

On the other hand, modified PEGs with relatively long EO chains are widely used for cosmetics and paints in adjusting rheological properties. Therefore, it is practically interesting, as well as from scientific aspects, to understand micelle formation, and the aggregation behavior of the modified PEGs with longer EO chains in aqueous solution.

Recently, we have investigated aqueous solutions of a modified PEG with relatively long EO chains, that is, PEG monododecyl ether (C12E25), over a wide range of concentration by static and dynamic light scattering, X-ray scattering, and linear viscoelasticity [21]. It is found that the micellar solution exhibits a disorder-to-order transition with increasing concentration, showing transitional changes in mechanical properties like a sol–gel transition. C12E25 is found to form star-like sphere micelles in dilute solution at 25 °C, and as increasing concentration, both of dynamic storage modulus G' and loss modulus G'' abruptly increase at a certain concentration (about 30 wt%), with G' dominating G'', which clearly shows a change to the gel, an elastic body. X-ray scattering indicates an ordered structure for the gel.

In this study, we investigate temperature dependencies of solution properties as well as the concentration dependencies for C12E25 aqueous solution to obtain the concentration–temperature diagram of the sol–gel transition due to disorder-to-order transition and understand more details of the transition. We have measured light scattering, linear viscoelasticity, and X-ray scattering for the solutions, and have clearly found the transition at about 56 °C with increasing temperature. We discuss the aggregation or condensed structure of micelles relating to temperature and concentration dependencies of linear viscoelastic properties.

* Corresponding author. Tel.: +81-3-5630-9426; fax: +81-5630-9339.
E-mail address: yamazaki.ritsuko@kao.co.jp (R. Yamazaki).
[1] Present address: Department of Materials Science and Engineering, Nagoya Institute of Technology, Gokiso-cho, Showa-ku, Nagoya 466-8555, Japan.
[2] Present address: Department of Applied Chemistry, Tokyo Institute of Polytechnics, Iiyama, Atsugi-shi, Kanagawa 243-0297, Japan.

PII: S0032-3861(02)00168-4

2. Experiments

2.1. Materials and samples

PEG monododecyl ether (C12E25) was an extra pure product of Tokyo-Kasei and used without further purification. Distilled water, a grade product of Wako Pure Medicine Co., was filterated and de-ionized by a Milli-Q Jr. (Millipore Co.). The specific resistance of the water was kept at 18.3 MΩ cm. Sample aqueous solutions were prepared as follows. Solutions of C12E25 with desired concentrations ranging from 0.5 to 60 wt% were homogenized by stirring for 3 h at 70 °C, and cooled down to room temperature. The prepared solutions were left for 1 day more.

2.2. Measurements

2.2.1. Light scattering

Apparatus and procedure. Light scattering was measured by a laboratory-made apparatus equipped with an ALV/SO-SIPD detector and an ALV-5000 correlator using a He–Ne laser (the wavelength λ of 633 nm) as a light source. Sample solutions were optically purified by a Millipore filter of nominal pore size of 0.2 μm, transferred into optical tubes, and were flame-sealed under mild vacuum. The measurements were carried out for a dilute solution (0.056 g/ml) at temperatures of 25–80 °C.

Data analyses. The excess Rayleigh ratio $R(q)$ as a function of wave number (q), which is defined by $q = (4\pi n/\lambda)\sin(\theta/2)$ with scattering angle θ, and refractive index n, was analyzed to determine the apparent molecular weight M_{wapp} by Zimm-type plots. Namely, the extrapolation of $KC/R(q)$ vs. q^2 plot to the zero q yields the value of $1/M_{wapp}$ at finite concentrations, where the constant K is given by $K = 4\pi^2 n^2 (\delta n/\delta c)^2/(N_A \lambda^4)$, with N_A being the Avogadro constant, and C is the concentration. The refractive index increment, $\delta n/\delta c$, of C12E25 was measured by a differential refractometer (UNION Giken RM-102) to be 0.144 ml/g at 25 °C. The excess Rayleigh ratio $R(q)$ was evaluated by using the value of benzene as standard. The Rayleigh rate of benzene was calculated by the equation [22]:

$$R(\theta = 90°)\, m^{-1} = 9.89 \times 10^{-7}[1 + 8.215 \times 10^{-3}(t - 30)]$$

(t : temperature °C) (1)

Dynamic light scattering. Dynamic light scattering was measured at 90° in most cases. The correlation function, $G^{(1)}(t)$, of electric field was calculated from the autocorrelation function, $G^{(2)}(t)$, of scattered light intensity by the equation

$$G^{(2)}(t) = A[1 + B|G^{(1)}(t)|^2] \quad (2)$$

where A and B are constants. $G^{(1)}(t)$ is approximately followed a single-exponential decay and allowed us to obtain the decay rate, Γ, by the second-order cumulant method. The Γ value showed q^2 dependence, so that the diffusion coefficient D was evaluated by $D = \Gamma/q^2$. The obtained D was transformed to the hydrodynamic radius, R_h, by the Einstein–Stokes equation,

$$R_h = k_B T/(6\pi\eta D) \quad (3)$$

Here, k_B is the Boltzmann constant, and η is the solvent viscosity.

2.2.2. Measurements of dynamic viscoelasticity

The dynamic viscoelasticity was measured with an ARES viscoelastic measuring apparatus (Rheometrics) using rotators of cone-plate geometry (diameter: 25 mm, angle: 0.04 rad). In order to prevent solvent, water, from evaporating, a specially designed sample cover was made and properly installed surrounding the rotators holding sample solution. No detectable evaporation was found for several hours at temperatures up to 60 °C. All the measurements were carried out within the linear viscoelasticity, which was confirmed by no strain dependence of the dynamic storage modulus G' and loss modulus G''. The strain γ ranged from 0.001 to 0.1 depending on the concentration of solution. The dynamic modulus was measured as a function of frequency, ω, ranging 0.1–100 s^{-1} at various temperatures of 25–70 °C for the solutions with different concentrations of 20–50 wt%.

2.2.3. X-ray scattering measurement

Wide angle X-ray scattering (WAXS) measurements were performed with a X-ray generator RU-200BH (RIGAKU Co.) at 25 and 80 °C. Cu Kα beam (wavelength $\lambda = 0.154$ nm, power: 4 kW) monochromatized by filtering through Ni was radiated to sample solution inserted into capillary tubes with 1.5 mm diameter for 10 min, and the scattered X-ray intensity was integrated on an imaging plate detector. One-dimensional scattering profiles were obtained by circularly averaging the two dimensional scattering pattern of intensity on the imaging plate.

3. Experimental results

3.1. Micellization in dilute aqueous solution observed by light scattering

Fig. 1 shows the temperature dependence of the apparent aggregation number, N_{app}, calculated from M_{wapp}, which indicates that N_{app} was about 26 being constant in the range 25–80 °C. The hydrodynamic radius is $R_{happ} = 3.0(\pm 0.2)$ nm irrespective of temperature. Considering the value of N_{app} and the particle size, C12E25 molecules are believed to be forming star-like spherical micelles by association in aqueous solution, and the micelles are stable in the present temperature range without appreciable change of the aggregation number.

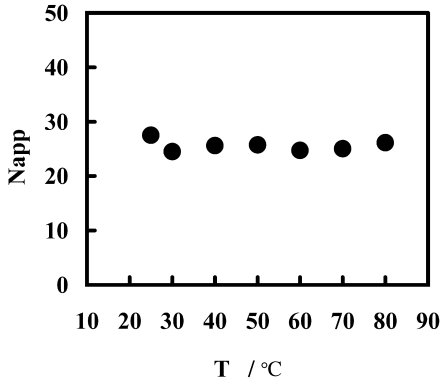

Fig. 1. Apparent association number, N_{app}, as a function of temperature for the C12E25 dilute aqueous solution of 0.0056 g/ml.

3.2. Concentration dependencies of the linear viscoelasticity

In Fig. 2 are shown log–log plots of G' and G'' vs. frequency ω for C12E25 aqueous solutions with various concentrations at 40 °C. As the concentration increases, the modulus G' increases, showing an abrupt change between 28 and 30 wt%, and becomes less dependent on ω. At lower concentrations, G'' is much larger than G', with the slope of G''–ω being about unity, which indicates that the C12E25 aqueous solution behaves as a viscous liquid. The elastic modulus G' for the higher concentration of 50 wt% shows a plateau region having a low loss modulus G''. Here the C12E25 aqueous solution is rubbery, i.e. gel-like in the frequency range of $0.1 < \omega < 10\ s^{-1}$.

Fig. 3 shows concentration dependencies of the storage modulus G' and the loss modulus G'' at the fixed frequency $\omega = 15.8\ s^{-1}$ for C12E25 aqueous solution at different temperatures, 25 and 40 °C. Around 30 wt%, G' and G'' sharply increase with increasing concentration by 10^{6-8} times of the order of magnitude, exhibiting a transitional change of the solution from a viscous liquid to a viscoelastic solid. That is, it is a sol-to-gel transition: G' dominates over G'' in the gel, while G'' is about 10^2 times larger than G' in the sol. The transition concentration has no practical difference between 25 and 40 °C, although the moduli are lower at the higher temperature in each of sol and gel regions.

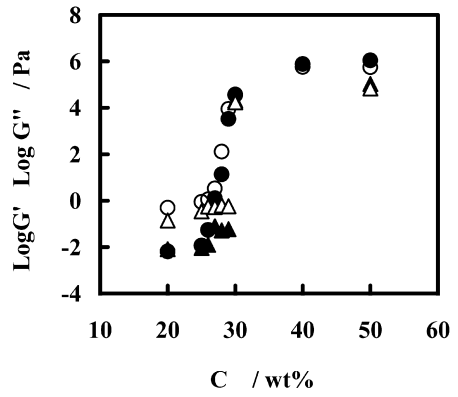

Fig. 3. G' and G'' at $\omega = 15.8\ s^{-1}$ against concentration for C12E25 aqueous solution at 25 °C (G': filled circles, G'': hollow circles) and 40 °C (G': filled triangles, G'': hollow triangles).

3.3. Temperature dependency of the linear viscoelasticity

In Fig. 4 are shown log–log plots of G' and G'' vs. frequency ω for C12E25 40 wt% aqueous solution at various temperatures. As the temperature decreases, G' increases, and the ω-dependence of G' becomes weaker. At higher temperatures, G'' is much larger than G', with the slope of G'' (ω) profile being about unity, which implies that the C12E25 aqueous solution behaves as a viscous liquid. At lower temperatures, the elastic modulus, G', has a plateau region with low loss modulus G''. Here, the

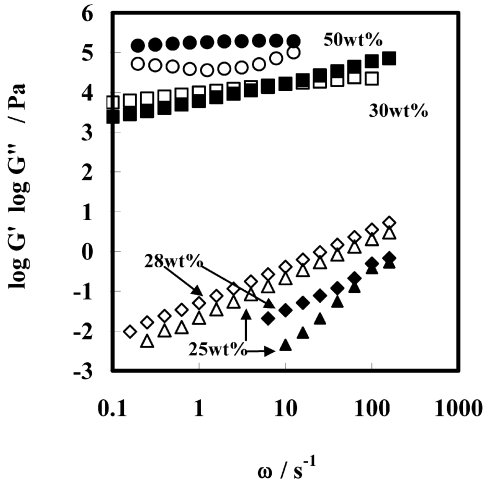

Fig. 2. Log–log plots of dynamic moduli G' (filled symbols) and G'' (hollow symbols) against frequency ω for C12E25 aqueous solutions of various concentrations indicated at 40 °C.

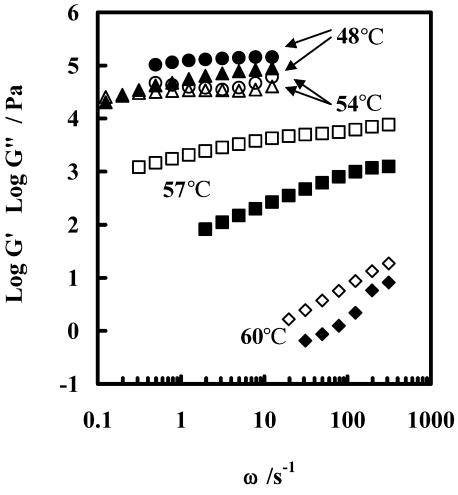

Fig. 4. Log–log plots of dynamic moduli G' (filled symbols) and G'' (hollow symbols) against frequency ω for the C12E25 aqueous solution of 40 wt% at various temperatures indicated.

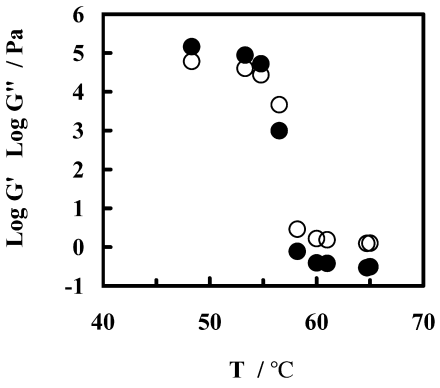

Fig. 5. Temperature dependencies of G' (filled circles) and G'' (hollow circles) at $\omega = 15.8\ s^{-1}$ for the C12E25 aqueous solution of 40 wt%.

C12E25 aqueous solution is rubbery, i.e. gel-like in the frequency range of $1 < \omega < 100\ s^{-1}$.

Fig. 5 represents temperature dependencies of G' and G'' at $\omega = 12.8\ s^{-1}$ for C12E25 40 wt% aqueous solution. Both G' and G'' dramatically decrease with increasing temperature, especially G' changes by about six orders of magnitude in the narrow temperature range of 54–56 °C. This demonstrates the occurrence of gel-to-sol transition. The sharp change more clearly appears in the tan δ vs. temperature plots in Fig. 6. At 56 °C, tan δ discontinuously changes from 0.5 to 5 with increasing temperature, which can determine the transition temperature to be 56 °C.

In Fig. 7, are plotted G'' at $\omega = 12.8\ s^{-1}$ for C12E25 aqueous solutions with various concentrations against the temperature T. At concentrations higher than the transition concentration of 30 wt%, G'' shows a sharp transition around 55 °C. It is noted that the G''–T relation is almost independent of the concentration, which implies that the transition temperature is independent of concentration.

On the other hand, G'' at 30 wt%, the transition concentration, decreases much more gradually than those at higher concentrations with increasing temperature, although the values of G'' at lower temperatures are almost equal to those for more concentrated solutions.

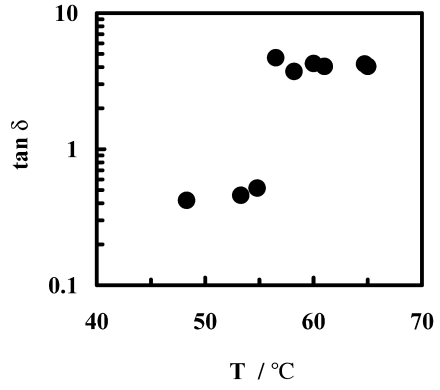

Fig. 6. Temperature dependence of tan δ at $\omega = 15.8\ s^{-1}$ for the C12E25 aqueous solution of 40 wt%.

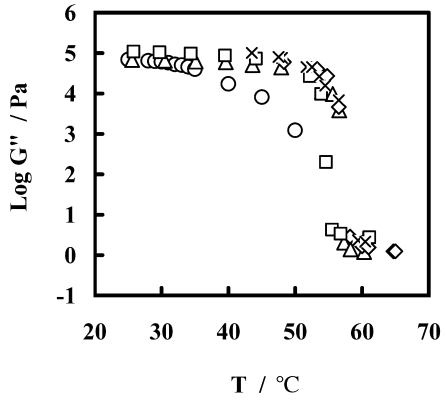

Fig. 7. Temperature dependency of G'' at $\omega = 15.8\ s^{-1}$ for C12E25 aqueous solutions of various concentrations indicated.

Summarizing the above results, we can draw the concentration–temperature diagram for sol and gel regions shown in Fig. 8, where the boundary between sol and gel regions, the so-called gelation point, is defined as the point of $G' = G''$ at $\omega = 15.8\ s^{-1}$.

3.4. Wide-angle X-ray scattering for concentrated C12E25 aqueous solution

WAXS profiles at 25 and 80 °C are shown for the C12E25 aqueous solution of 25 and 40 wt% in Fig. 9(a) and (b), respectively.

At 25 wt%, which is below the transition concentration, there appears only one broad peak at the wave-number $q_1 = 1.5\ nm^{-1}$ at 25 °C, and at $q_1 = 1.2\ nm^{-1}$ at 80 °C. Similarly, one sees only one broad peak at $q_1 = 1.0\ nm^{-1}$ accompanied with a shoulder at higher q region at the higher concentration 40 wt% in the sol region, at 80 °C. To the contrary, in the gel region, at 40 wt% and 25 °C, a strong sharp diffraction peak is found at $q_1 = 0.96\ nm^{-1}$ with the higher order diffraction peaks; the second peak at $q_2 = 1.40\ nm^{-1}$, and the third peak at $q_3 = 1.69\ nm^{-1}$. The ratios of peak positions among these peaks are $q_1/q_2/q_3 = 1 : 2^{1/2} : 3^{1/2}$, indicating that the C12E25 gel has a long-range

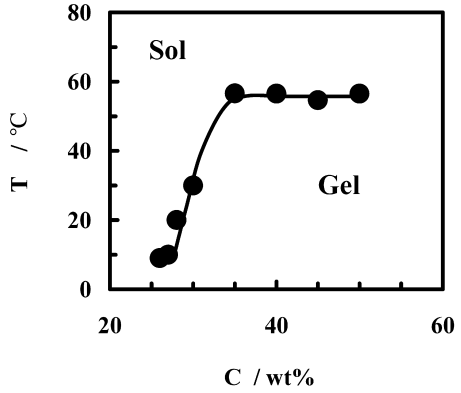

Fig. 8. Concentration–temperature (C–T) diagram of sol and gel regions for the C12E25 aqueous solution.

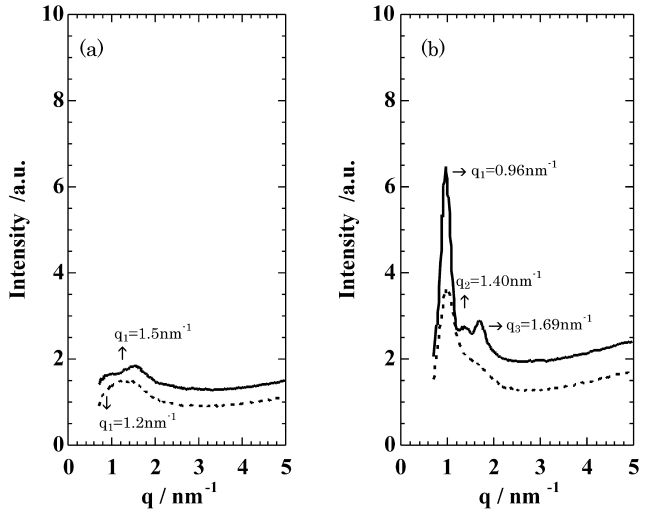

Fig. 9. X-ray scattering profiles for C12E25 aqueous solutions at 25 °C (solid lines) and 80 °C (dashed lines). (a) 25 and (b) 40 wt%.

order structure with body-centered cubic lattice. The distance between nearest-neighbor particles is calculated from the lattice constant to be 7.9 nm.

4. Discussion

In summarizing the experimental results, C12E25 forms rather stable star-like micelles with the association number being about 26 in the whole range of temperature.

At higher concentrations and lower temperatures, i.e. above 30 wt% and below 56 °C, there exists the gel region, where the micelles construct an ordered structure having a body-centered cubic lattice. The micelle size is 6 nm or larger in diameter, yielding the nearest-neighbor distance of about 8 nm in the ordered state. The gel is really elastic, having the elastic shear modulus of 1×10^5 Pa, in the frequency range 1–100 s^{-1}. The sol–gel transition accompanied with disorder-to-order transition occurs sharply, and the transition concentration is independent of temperature. This seems quite natural, because the occurrence of the order–disorder transition of colloidal particles such as Alder transition is usually primarily controlled by the volume fraction of particles, being very weakly dependent on temperature. However, in the present case, there exists a sharp gel-to-sol transition with increasing temperature, and furthermore the transition temperature is almost independent of concentration. Reminding that no appreciable change is found in the association number of micelles over the whole temperature range, very delicate conditions are controlling the stability of ordered lattice. Slight changes in nature of long arm EO chains with temperature might play an important role in the stability of the ordered state.

Lattice structures similar to the present observation were reported for spherical micelle solutions of diblock copolymers and those of triblock copolymers of purulonic-types (polyethyleneoxide–polypropyleneoxide–polyethyleneoxide) [23–26]. Aqueous solution of 28 wt% purulonic triblock polymers (F88 M_w 11800) is reported to have the sol–gel transition temperature, at which the solution changes from a sol of micellar disordered structure to a gel with an ordered arrangement of micelles [23]. Watanabe et al. reported that polystyrene–polybutadiene diblock polymer forms micelles in tetradecane solution, and the micelles are aligned in lattice order [24,25,27,28]. Watanabe et al. found that polystyrene–polybutadiene diblock polymer forms micelles in tetradecane solution, and the micelles are aligned in lattice order [24,25,27,28]. Furthermore, they demonstrated that the elastic modulus G_e is proportional to the number density of the corona blocks in the micellar lattice, and reported that the proportionality suggests that the osmotically constrained corona blocks entropically sustain the equilibrium elasticity.

5. Conclusions

Aggregation behavior of hydrophobically modified ethylene–glycol oligomer C12E25 in aqueous solution has been studied in wide ranges of concentration and temperature. C12E25 is found to form stable star-like micelles in dilute solution in the temperature range 25–80 °C. With increasing concentration at lower temperatures, or with decreasing temperature at higher concentrations, the micellar solution exhibits the sol–gel transition accompanied with disorder-to-ordered structural transition. At the transition, the solution changes drastically from a viscous liquid to a viscoelastic solid. The micellar particles form a long-range order structure of body-centered cubic in the gel region. The transition concentration is 30 wt% irrespective of temperature, while the transition temperature is 56 °C independent of concentration.

References

[1] Shinoda K. J Colloid Interface Sci 1970;34:278.
[2] Mitchell DJ, Tiddi DJT, Waring L, Bostock T, McDonald MP. J Chem Soc, Faraday Trans 1983;79:975.
[3] Lang LC, Morgan RD. J Chem Phys 1980;73:5849.
[4] Zulauf Z, Rosenbusch JP. J Phys Chem 1983;87:856.
[5] Corti M, Minero C, Degiorgio V. J Phys Chem 1984;88:309.
[6] Corti M, Minero C, Cantu L, Piazza R. Colloids Surf 1984;12:34.
[7] Meguro K. J Oil Chem 1998;37:228.
[8] Tanfoed C, Nozaki Y, Rohde MF. J Phys Chem 1977;81:1555.
[9] Corkill JM, Walker T. J Colloid Interface Sci 1972;39:621.
[10] Kato T, Seimiya T. J Phys Chem 1986;90:3159.
[11] Honda C, Kuchi Y, Nose T. J Chem Soc 1992;11:1301.
[12] Attwood D. J Phys Chem 1968;72:339.
[13] Brown W, Johnsen RM, Stilbs P. J Phys Chem 1983;87:4548.
[14] Brown W, Rymden R. J Phys Chem 1987;91:3565.
[15] Zana R, Weill C. J Phys (Paris) Lett 1985;46:L-953.
[16] Kato T, Anzai S, Seimiya T. J Phys Chem 1990;94:7255.
[17] Imae T. J Phys Chem 1988;92:5721.
[18] Kato T. J Oil Chem 1992;41:75.
[19] Nilsson PG, Lindman B. J Phys Chem 1983;87:4756.

[20] Nilsson PG, Wennerstrom H, Lindman B. J Phys Chem 1983;87:1377.
[21] Yamazaki R, Inomata K, Nose T. Kobunshi Ronbunshu 2001;58:286.
[22] Nose T, Chu B. Macromolecules 1979;12:590.
[23] Mortensen K. Prog Colloid Polym Sci 1993;91:69.
[24] Watanabe H, Kotaka T, Hashimoto T, Shibayama M. J Rheol 1982;26:153.
[25] Watanabe H, Kotaka T. Polym Engng Rev 1984;4:73.
[26] Shibayama M, Hashimoto T, Kawai H. Macromolecules 1993;26:4935.
[27] Watanabe H, Kanaya T, Takahashi Y. Macromolecules 2001;34:662.
[28] Watanabe H. Acta Polym 1997;48:215.